

GT2011-45078

INVESTIGATION OF TURBULENT MODELS FOR THE FLOW FIELD FROM A TYPICAL STRUT-BASED SCRAMJET COMBUSTOR

Shi-bin Luo, Wei Huang*, Hui Qin, Zhen-guo
Wang, Jun Liu, Zhi-xun Xia, Jing Lei
Center of Hypersonic Propulsion
College of Aerospace and Materials Engineering
National University of Defense Technology
Changsha, Hunan, 410073, China

Mohamed Pourkashanian, Lin Ma,
Derek B.Ingham, Wen-lei Luo†
Centre for CFD
School of Process, Environmental and Materials
Engineering
University of Leeds
Leeds, LS2 9JT, United Kingdom

ABSTRACT

The two-dimensional coupled implicit RANS equations and three turbulent models have been employed to numerically simulate the nonreacting and reacting flow fields of a typical strut-based scramjet combustor, and the numerical results have been compared with the experimental data. At the same time, three different grid scales have been used to test the grid independence in the numerical simulations, namely the small scale (81,590 nodes), the moderate scale (98,510 nodes) and the large scale (147,470 nodes). The obtained results show that the RNG $k-\epsilon$ model is more suitable to numerically simulate the flow field in the scramjet combustor than the realizable $k-\epsilon$ model and the SST $k-\omega$ model, and the numerical results obtained by the moderate and large grid scales show reasonably better agreement with the experimental data. The quasi-diamond wave system is formed in both the nonreacting and reacting flow fields. In the reacting flow field, there are two clear strong shear layers generated between the fuel injection and the supersonic freestream, and at the intersection point between the shear layer and the reflected shock wave, the reaction zone is broader than anywhere else. In the corner formed between the upper surface of the strut and the shear layer, an expansion wave is clearly generated, and another also exists in the symmetrical corner.

INTRODUCTION

Recently, as one of the most promising hypersonic airbreathing propulsion systems, the scramjet engine has drawn an ever increasing attention of researchers worldwide, and it

can satisfy the military requirement of a long-range strike capability[1]. However, there are still numerous important critical techniques to be dealt with, e.g. improving the mixing efficiency between the fuel and the air in the supersonic environment, keeping the flame stable and prolonging the residence time[2-5]. In order to make the fuel and the supersonic airstream mix more efficiently, the strut is used widely in the scramjet combustor as the fuel injector, and the fuel is injected from the base surface of the strut horizontally[6-10]. There is a pair of axial vortices generated in the vicinity of the base surface, and the axial vortices are separated by the fuel injection. The axial vortex plays an important role in improving the mixing efficiency in supersonic flow[6].

Further, as an effective tool in supporting costly ground experimental tests, Computational Fluid Dynamics methods have been employed widely to investigate the flow field in the scramjet engine. Gerlinger et al. [6] applied the inhouse TASC3D (Turbulent All Speed Combustion Multigrid) solver in the numerical simulations of a Mach 2 model scramjet combustor. Genin et al. [7] and Berglund et al. [9] used large-eddy simulation with a new localized dynamic subgrid closure to investigate the compressible turbulent mixing in a strut-based injection system. Oevermann et al. [8] employed a two equation $k-\epsilon$ turbulence model combined with a stretched laminar flamelet model to simulate the hydrogen injection in a scramjet engine. At the same time, the newly-proposed Partially Resolved Numerical Simulation (PRNS) procedure was introduced to simulation a DLR (German Aerospace Center) scramjet engine [10].

* Corresponding author, joint PhD student between National University of Defense Technology and University of Leeds, email: gladrain2001@yahoo.com.cn

† Joint PhD student between National University of Defense Technology and University of Leeds

However, in the open literature, there are still few papers to contrast the numerical predictions of the typical RANS models for the scramjet engines, even the strut-based combustor.

In this paper, the nonreacting and reacting flow fields of a typical strut-based scramjet combustor are numerically simulated, and the effect of the different turbulence models on the wave structure and parametric distributions in the combustor is discussed, namely the SST $k-\omega$, the realizable $k-\epsilon$ and the RNG $k-\epsilon$ models. At the same time, the grid independence was investigated by using three different grid scales, namely the large scale (147,470 nodes), the moderate scale (98,510 cells) and the small scale (81,590 cells), and the experimental data from the literature have been used to validate the accuracy of the numerical results.

PHYSICAL MODEL

The geometric model which has been built is based on a typical strut-based scramjet combustor, which is tested in the German Aerospace Center[6-9], see Fig.1. Preheated air is expanded through a laval nozzle and enters the combustor at Mach 2[9], and the combustor has a length 340mm and a height 50mm at the entrance. From $X = -9$ mm onwards, the upper wall of the combustor diverges at a constant angle of 3° to compensate for the boundary layer growth. A strut is placed at the centerline, namely $Y = 25$ mm. The length of the strut is 32mm, and its half-angle is 6° . The hydrogen is injected horizontally from the centre of the strut base with local sonic velocity, the strut base is located at $X = 0$, and the width of the injection slot is 1mm.

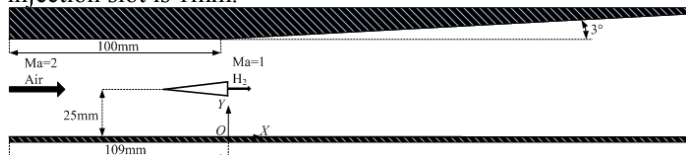


Figure 1. A schematic of a typical strut-based scramjet combustor.

The static pressure and temperature of the hypersonic inflow are 100,000Pa and 340K, respectively. At the same time, the static pressure and temperature of the fuel are 100,000Pa and 250K, respectively.

NUMERICAL METHODS

Three different turbulent models have been employed to investigate the nonreacting and reacting flow fields of the typical strut-based scramjet combustor, namely the SST $k-\omega$, the realizable $k-\epsilon$ and the RNG $k-\epsilon$ models[11]. Considering the strength of the turbulent combustion, the finite-rate/eddy-dissipation reaction model has been introduced to simulate the reacting flow field of the combustor[3]. Because this paper mainly investigates the effect of the turbulent models on the flow field of the combustor, the effect of the more complex chemical dynamic reactions will be discussed in the future, the single step chemical reaction of hydrogen combustion is applied in this paper, and the reaction equation is as follows:



A structured grid is employed for the configuration. The grid is generated using the commercial software Gambit, and the grid is refined near the wall of the combustor, in the vicinity of the injection slot, see Fig.2. Fig.2 shows a schematic of grid system for the moderate scale, and the height of the first row of cells is set at a distance to the wall of 0.01mm. At the same time, three grid scales are employed to investigate the grid independence in the numerical simulations, namely 81,590, 98,510 and 147,470 cells.

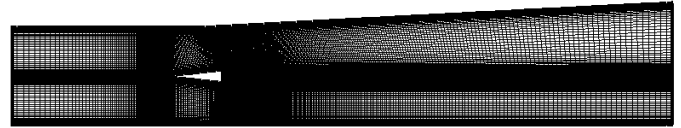


Figure 2. A schematic of grid system for the moderate scale.

RESULTS AND DISCUSSION

Nonreacting flow field

Fig.3 shows the static pressure distributions along the lower wall of the scramjet combustor under the condition of cold flow by using different grid scales, namely the small scale (81,590 nodes), the moderate scale (98,510 nodes) and the large scale (147,470 nodes), and the numerical results are obtained by using the RNG $k-\epsilon$ model. We can observe that the numerical results obtained by the moderate and large scales show reasonably better agreement with the experimental data than the small scale, and the discrepancy between the numerical results obtained by the moderate and large scales is only small. The pressure increases because of the generation of the shock wave, and the third shock wave location obtained by the experiment is a bit later than the numerical prediction. In Fig.3, the experimental data after the second shock wave location are not provided.

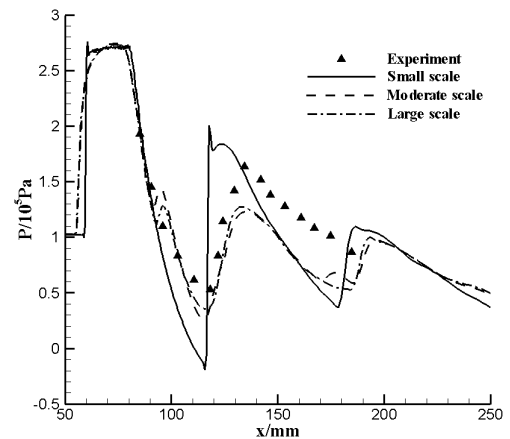


Figure 3. Pressure distributions along the lower wall of the scramjet combustor without combustion which are obtained with three different grid scales.

At the same time, in the vicinity of the base surface of the strut, along the lower wall of the scramjet combustor, the numerical result obtained by the moderate scale shows good agreement with that obtained by the small one, even the highest static pressure. Therefore, the moderate grid scale is employed in the following numerical simulations.

Fig.4 shows a comparison of the pressure distributions along the lower wall of the combustor under the condition of cold flow by using different turbulent models, and the numerical result obtained by the RNG k-ε model shows better agreement with the experimental data than the other two models, namely the realizable k-ε model and the SST k-ω model.

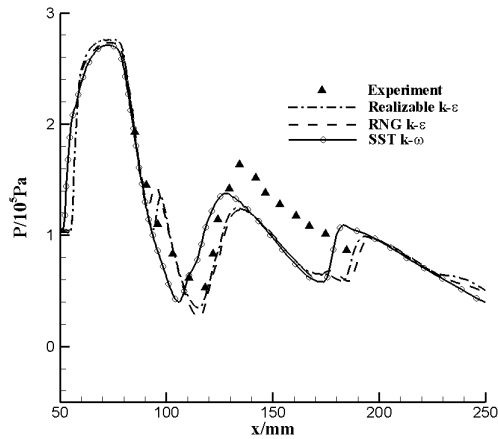


Figure 4. Pressure distributions along the lower wall of the scramjet combustor without combustion which are obtained with three different turbulent models.

Fig.5 and Fig.6 show the static pressure and Mach number contours of the scramjet combustor without combustion which is obtained by using the RNG k-ε model, respectively. It is clearly that several quasi-diamond shock waves are generated in the flow field of the combustor, see Fig.5, and because of the

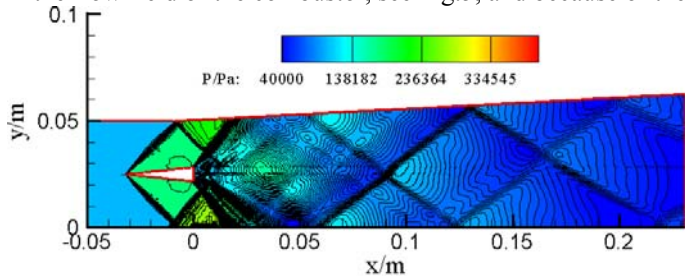


Figure 5. Pressure contour of the scramjet combustor without combustion.

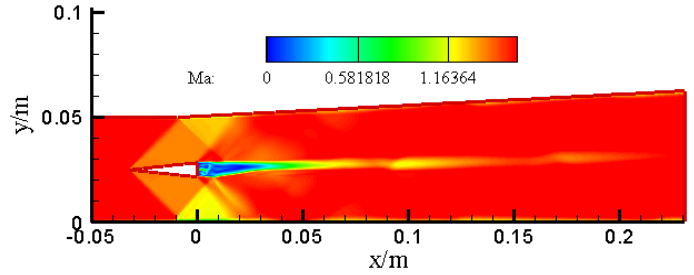
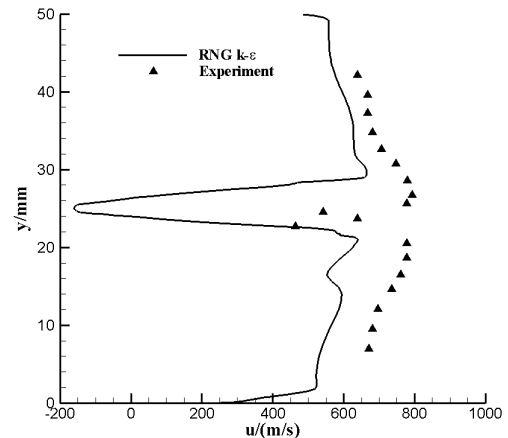


Figure 6. Mach number contour of the scramjet combustor without combustion.

divergent angle of the upper wall of the combustor, the quasi-diamond shock waves are not symmetric.

At the same time, there are two strong oblique shock waves formed at the tip of the strut, see Fig.5, and two weak shear layers are generated between the injection and the supersonic freestream in the vicinity of the base surface of the strut, see Fig.6. Because of the generation of the shear layers, an expansion wave is formed in the corner between the upper surface of the strut and the shear layer, and another also exists in the symmetrical corner. A low velocity region, which is called the recirculation zone, is formed near the base surface of the strut, and this is because of the generation of two eddies between the injection and the shear layers.

Fig.7 shows the cross-stream velocity profiles at different streamwise locations x which are obtained by using the RNG k-ε model, namely $x = 11\text{mm}$, 58mm , 90mm and 166mm , and the numerical results show reasonably good agreement with the experimental data. There are some discrepancies between the numerical results and the experimental data which may be caused by the two-dimensional simulation and the discrepancies between the experimental setting and the



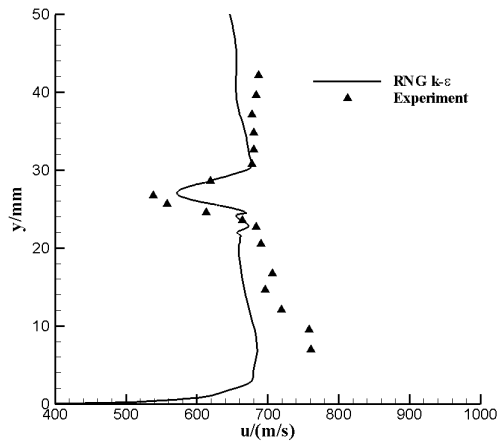
(a) $x=11\text{mm}$

boundary conditions employed in the numerical simulations, and the numerical results are underestimated.

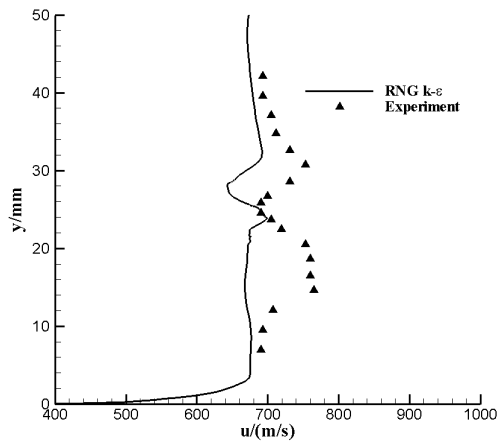
Reacting flow field

Fig.8 and Fig.9 show the cross-stream velocity profiles and the cross-stream static temperature profiles at three different streamwise locations x , respectively, in Fig.8, $x = 11\text{mm}$, 58mm and 140mm , and in Fig.9, $x = 11\text{mm}$, 58mm and 166mm . There are some discrepancies between the numerical results and the experimental data as well, and the cross-stream velocities are underestimated, see Fig.8, but the cross-stream static temperature is slightly overestimated, see Fig.9. However, the numerical results show reasonably good agreement with the experimental data, and the discrepancies may be caused by the simulation being two-dimensional [10].

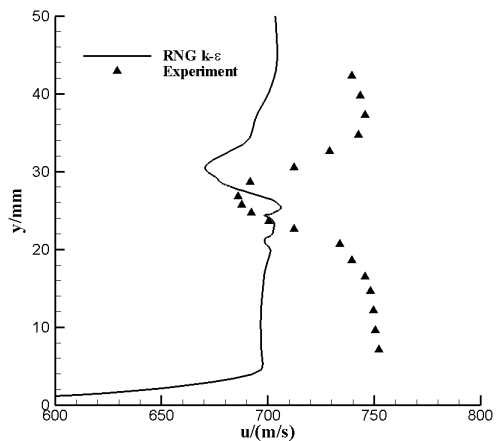
At the same time, in Fig.8, at $x = 11\text{mm}$ the qualitative and quantitative agreement between the numerical result and the experimental data is better than the other two locations, namely



(b) $x=58\text{mm}$

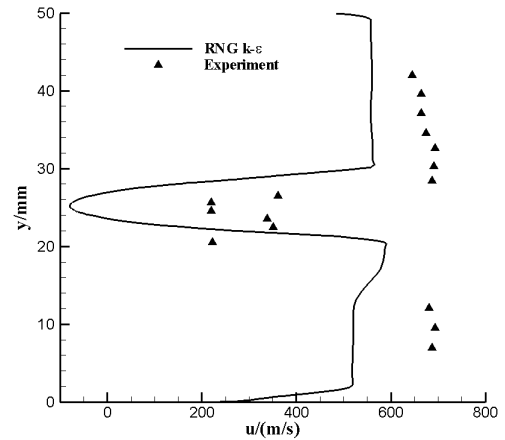


(c) $x=90\text{mm}$

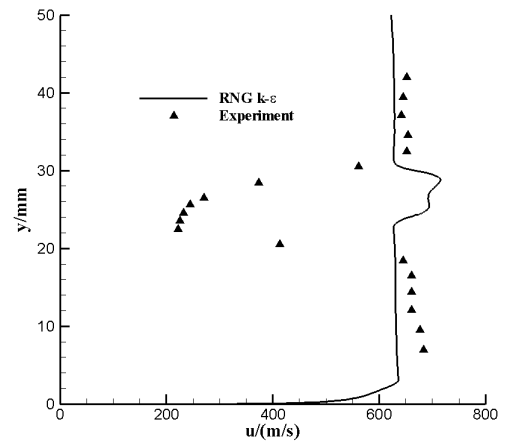


(d) $x=166\text{mm}$

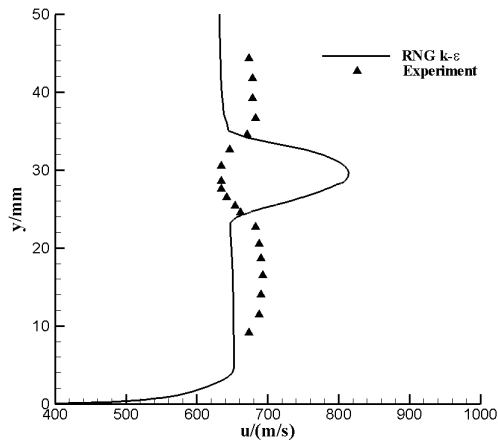
Figure 7. Cross-stream velocity profiles at different streamwise locations x .



(a) $x=11\text{mm}$

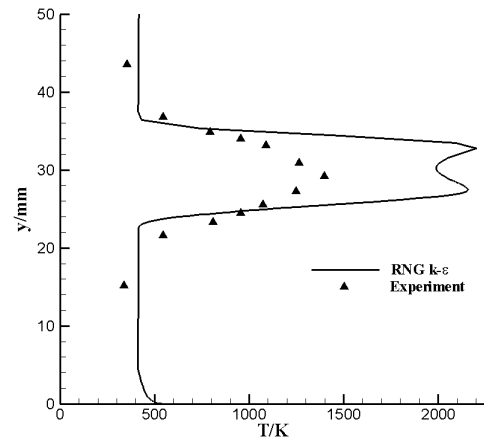


(b) $x=58\text{mm}$



(c) $x=140\text{mm}$

Figure 8. Cross-stream velocity profiles at three different streamwise cross-sections x .

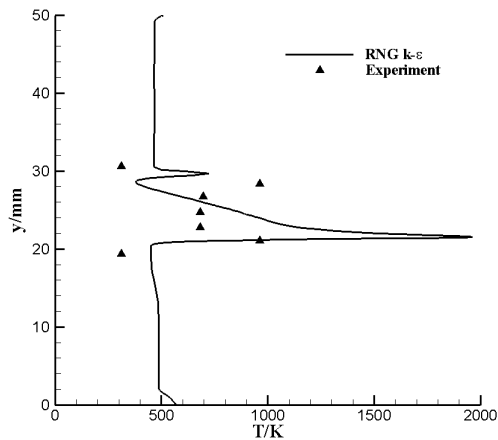


(c) $x=166\text{mm}$

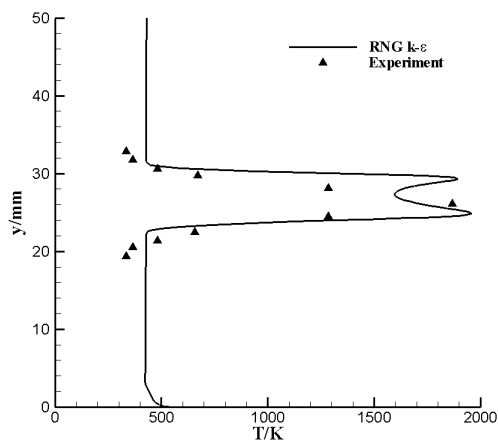
Figure 9. Cross-stream static temperature profiles at three different streamwise locations x .

Fig.8 (b) and (c). Further downstream at $x = 58\text{mm}$ and $x = 140\text{mm}$ the long acceleration of the fuel stream in the simulation leads to velocities of the inner jet higher than the surrounding upper and lower air stream, which contrasts with the experimental observation [8].

Fig.10 and Fig.11 show the static pressure and the Mach number contours of the scramjet combustor with combustion, respectively, and because of the intense combustion, the static pressure is much higher than that in the nonreacting flow field, see Fig.10. The quasi-diamond wave system is broken down by the intense combustion, and the shock waves generated in the vicinity of the strut are much stronger. The effect of the expansion wave on the shock wave and the reflected one is weak. At the same time, the shear layers formed between the



(a) $x=11\text{mm}$



(b) $x=58\text{mm}$

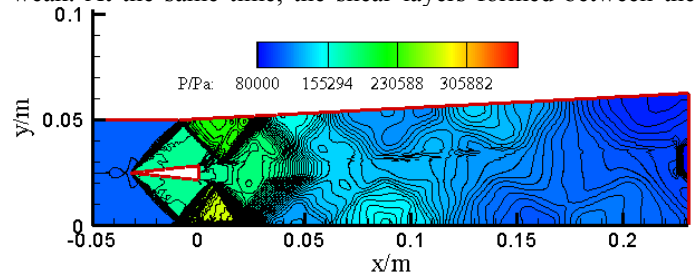


Figure 10. Pressure contour of the scramjet combustor with combustion.

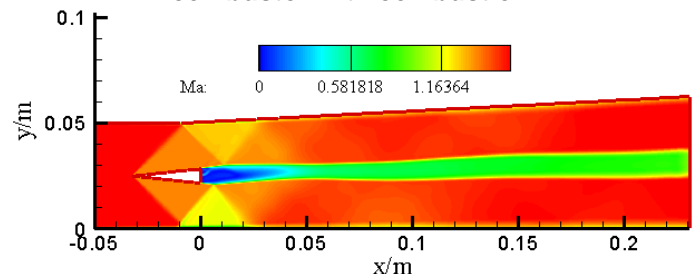


Figure 11. Mach number contour of the scramjet combustor with combustion.

injection and the supersonic freestream are clearer, in other words, the shear layers generated in the reacting flow field of the combustor are stronger. In the reacting flow field, the low velocity region generated in the vicinity of the base surface extends further downstream, see Fig.11.

At the intersection point between the shear layer and the reflected shock wave, the reaction zone is broader than anywhere else.

Fig.12 shows the H₂O mass fraction contour of the

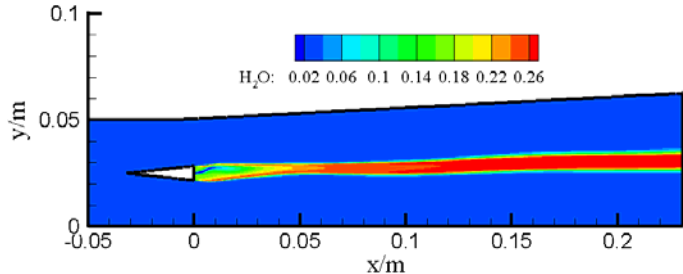


Figure 12. H₂O mass fraction contour of the scramjet combustor with combustion.

scramjet combustor with combustion, and the intense combustion occurs mainly along the centerline of the combustor, even after $x = 50\text{mm}$.

CONCLUSIONS

In this paper, three turbulent models are employed to investigate the nonreacting and reacting flow fields of a typical strut-based scramjet combustor, namely the RNG $k-\epsilon$ model, the realizable $k-\epsilon$ model and the SST $k-\omega$ model, and three different grid scales are used to validate the grid independence in the numerical simulations, namely the large scale (147,470 cells), the moderate scale (98,510 cells) and the small scale (81,590 cells). We observe the following:

- The RNG $k-\epsilon$ model is more suitable to numerically simulate the flow field of the typical strut-based scramjet combustor than the realizable $k-\epsilon$ model and the SST $k-\omega$ model. It is likely that the discrepancy between the numerical results and the experimental data is generated because the simulations are two-dimensional and there are some discrepancies exist between the experimental setting and the boundary conditions employed in the numerical simulations.
- The numerical results obtained from the moderate and large scales show better agreement with the experimental data than that obtained from the small grid scale, and the discrepancies between the numerical results obtained by the moderate and large scales are only small. At the same time, the grid scale makes only a slight difference to the pressure distribution in the vicinity of the base surface of the strut.
- In the reacting flow field, the reaction zone at the intersection point between the shear layer and the reflected shock wave is broader than anywhere else,

and the quasi-diamond wave system is broken down because of the intense combustion.

- Two clear shear layers are generated in the reacting flow field of the scramjet combustor, and the low velocity region extends further downstream.

ACKNOWLEDGMENTS

The second author would like to express his sincere thanks for the support from the National Science Foundation of China (No.90816027), the Excellent Graduate Student Innovative Project of the National University of Defense Technology (No.B070101), the Hunan Provincial Innovation Foundation for Postgraduate (No.3206), and the Chinese Scholarship Council (CSC) for their financial support (No.2009611036). Also the authors would like to thank the reviewers for some very constructive recommendations on the draft of this paper.

REFERENCES

- [1] Waltrup PJ, White ME, Zarlino F, Gravlin ES. History of ramjet and scramjet propulsion development for U.S. navy missiles. Johns Hopkins Apl Technical Digest 1997;18(2):234-243.
- [2] Huang W, Qin H, Luo S-b, Wang Z-g. Research status about key techniques of shock-induced combustion ramjet (shcramjet) engine. Science China Technological Sciences 2010;53(1):220-226.
- [3] Huang W, Luo S-b, Liu J, Wang Z-g. Effect of cavity flame holder configuration on combustion flow field performance of integrated hypersonic vehicle. Science China Technological Sciences 2010;53(10):2725-2733
- [4] Huang W, Luo S-b, Wang Z-g. Key techniques and prospect of near-space hypersonic vehicle (in Chinese). Journal of Astronautics 2010;31(5):1259-1265.
- [5] Huang W, Luo S-b, Pourkashanian M, Ma L, B.Ingham D, Liu J, Wang Z-g. Numerical simulations of a typical hydrogen fueled scramjet combustor with a cavity flameholder. The 2010 International Conference of Mechanical Engineering (WCE 2010), London, UK, 2010, p 1000-1003.
- [6] Gerlinger P, Stoll P, Kindler M, Schneider F, Aigner M. Numerical investigation of mixing and combustion enhancement in supersonic combustors by strut induced streamwise vorticity. Aerospace Science and Technology 2008;12(2):159-168.
- [7] Genin F, Menon S. Simulation of turbulent mixing behind a strut injector in supersonic flow. AIAA Journal 2010;48(3):526-539.
- [8] Oevermann M. Numerical investigation of turbulent hydrogen combustion in a SCRAMJET using flamelet modeling. Aerospace Science and Technology 2000;4(7):463-480.
- [9] Berglund M, Fureby C. LES of supersonic combustion in a scramjet engine model. Proceeding of the Combustion Institute 2007;31(2):2497-2504.

[10] Zou JF, Zheng Y, Liu OZ. Simulation of turbulent combustion in DLR scramjet. Journal of Zhejiang University SCIENCE A 2007;8(7):1053-1058.

[11] FLUENT I. FLUENT 6.3 User's Guide: Lebanon, NH: Fluent Inc; 2006.